Available online at www.sciencedirect.com
ScienceDirect
Journal of Theoretical Biology 251 (2008) 195–201
Journal of Theoretical Biology
www.elsevier.com/locate/yjtbi

A propagating heat wave model of skin electroporation

Uwe Pliquett[a,*], Ch. Gusbeth[b], Richard Nuccitelli[c]

[a]*Institut für Bioprozeß- und Analysenmeßtechnik e.V., D-37308 Heilbad Heiligenstadt, Germany*
[b]*Institut für Hochleistungsimpuls- und Mikrowellentechnik, Forschungszentrum Karlsruhe, Hermann-von-Helmholtz-Platz 1, D-76344 Eggenstein-Leopoldshafen, Germany*
[c]*BioElectroMed, 849 Mitten Road, Suite 105, Burlingame, CA, USA*

Received 5 March 2007; received in revised form 24 September 2007; accepted 21 November 2007
Available online 4 December 2007

Abstract

The main barrier to transdermal drug delivery in human skin is the stratum corneum. Pulsed electric fields (PEFs) of sufficient amplitude can create new aqueous pathways across this barrier and enhance drug delivery through the skin. Here, we describe a model of pore formation between adjacent corneocytes that predicts the following sequence of events: (1) the PEF rapidly charges the stratum corneum near the electrode until the transepidermal potential difference is large enough to drive water into a small region of the stratum corneum, creating new aqueous pathways. (2) PEFs then drive a high current density through this newly created electropore to generate Joule heating that warms the pore perimeter. (3) This temperature rise at the perimeter increases the probability of further electroporation there as the local sphingolipids reach their phase transition temperature. (4) This heat-generated wave of further electroporation propagates outward until the surface area of the pore becomes so large that the reduced current density no longer generates sufficient heat to reach the phase transition temperature of the sphingolipids. (5) Cooling and partial recovery occurs after the field pulse.

This process yields large, high permeability regions in the stratum corneum at which molecules can more readily cross this skin barrier. We present a model for this process that predicts that the initial radius of the first aqueous pathway is approximately 5 nm for a transdermal voltage of 60 V at room temperature.

Keywords: Skin electroporation; Lipid layer; Joule heating; Phase transition

1. Introduction

Transdermal drug delivery is enhanced by electroporation of the stratum corneum (SC), the most effective skin barrier to molecules and ions (Prausnitz et al., 1993; Weaver and Chizmadzhev, 1996). Electroporation itself is a non-thermal phenomenon at the level of the cell membrane. Once a membrane is charged to electroporation levels, water is forced into the lipid environment because of the large difference in dielectric constant ($\varepsilon_{water} \approx 87$, $\varepsilon_{lipid} \approx 2$). As soon as an aqueous channel (electropore) is created, the water inside the pore becomes polarized, thereby stabilizing the pore (Neumann et al., 1989). Since it is energetically unfavorable to have an interface of lipid tails and water inside the pores, it is expected that the lipids forming the pore edge orient with their head groups facing the pore, yielding a hydrophilic surface. A pore tends to expand during the presence of the electric field. It becomes stable if a critical pore radius is reached, even if the field is turned off. This change in the lipid environment persists for some time (Glaser et al., 1988). Pores that are below the critical radius recover quickly after the pulse (Chizmadzhev et al., 1995), and this may account for the partial recovery of the skin resistance found experimentally. Electroporation of the outer layer of skin, the SC, happens when $U_{SC} = 30$ V. The transport of medium-sized water-soluble molecules increases dramatically but is focused in localized transport regions (LTRs). The development of LTRs is not compatible with pure electroporation because they are always associated with local heating (Pliquett and Gusbeth, 2000).

*Corresponding author.
E-mail address: uwe.pliquett@iba-heiligenstadt.de (U. Pliquett).

0022-5193/$ - see front matter © 2007 Elsevier Ltd. All rights reserved.
doi:10.1016/j.jtbi.2007.11.031

All observations during the application of PEF are on the level of the whole SC. The electric field action, however, takes place mainly at the membrane level. Here, we investigate the changes at the membrane level by using experimental results together with simulation on the level of the multi-lamellae between adjacent corneocytes.

2. Experimental results on which the model is based

Our model is based upon the following experimental observations:

1. The central region of each LTR exhibits high permeability which decreases near the edges.
2. A sharp boundary separates the central region which exhibits essentially no recovery of the electrical resistance and the outer regions where recovery usually occurs (Pliquett et al., 1996; Prausnitz et al., 1996).
3. For pulsed field applications utilizing short pulses (<5 ms), the LTRs appear far from appendages like hair follicles and sweat glands. If pulses with a lower voltage ($U_{skin}<30$ V) but longer duration ($\tau>100$ ms) are applied, the LTRs often coincide with sweat ducts (Pliquett et al., 1998; Vanbever et al., 1999).
4. The density of LTRs is a function of the transdermal voltage difference. It starts with 1 LTR/cm^2 at $U_{skin}\approx 60$ V and approaches about 100 LTRs/cm^2 at $U_{skin}\approx 120$ V.
5. The size of LTRs is a clear function of the pulse duration. As the pulse duration increases from 1 to 100 ms, the LTR radius increases roughly linearly from 40 to 200 μm (Pliquett et al., 1998).
6. In all experiments assessing the time course of electroporation, a short pulse rise time of around 100 ns was used. The dramatic decrease in skin resistance occurs on the time scale of 1–10 μs (Pliquett et al., 1995).
7. A further slow decrease in skin resistance is due to either the enlargement of newly created pathways or the creation of even more pathways. Visualization of electroporation using fluorescent markers revealed no further LTR-creation after the first microseconds of the PEF.
8. The after-pulse recovery of the electrical skin resistance exhibits several steps from milliseconds up to hours (Pliquett et al., 1995) and spans a range of 20–98% (Pliquett and Gusbeth, 2000).
9. The rate of LTR heating during pulse application depends on both the duration of the pulse and the field strength. The temperature within the center regions reaches more than 70 °C, sufficient to exceed the phase transition temperature of the long-chain sphingolipids. The surrounding regions experience heating as well, but the temperature does not exceed 70 °C and a full recovery of the electrical resistance is observed after high field strength application (Pliquett and Gusbeth, 2000).

The phase transition temperature of long-chain sphingolipids in the SC is between 65 and 70 °C, depending on chain length and environment (Pliquett and Gusbeth, 2000). Below 70 °C a recovery of the resistance during cooling is observed. However, after exceeding 70 °C, the skin resistance stays permanently low at $0.2<R_{skin}$ (kΩ cm^2)<1, which is very similar to values found for LTR after electroporation.

The transdermal voltage necessary for electroporation is a function of temperature in the range between 0 and 60 °C. For human SC, electroporation occurs at a transdermal voltage difference of $80\text{ V}<U_{skin}<100$ V at 4 °C, while at 60 °C, $10\text{ V}<U_{skin}<20$ V will suffice.

2.1. Working hypothesis

The SC is composed of 6–15 layers of flattened, dead cells called corneocytes (Fig. 1) and exhibits the highest resistance of any skin layer. Our working hypothesis is that skin electroporation must first generate small pores in the SC in the regions between corneocytes, and this initiates a synergistic process in which current flow heats the SC, melting lipids to widen the pore resulting in more current flow. This differs from current thinking in which the observed heating is only a byproduct of current flow and is not involved in the electroporation process itself.

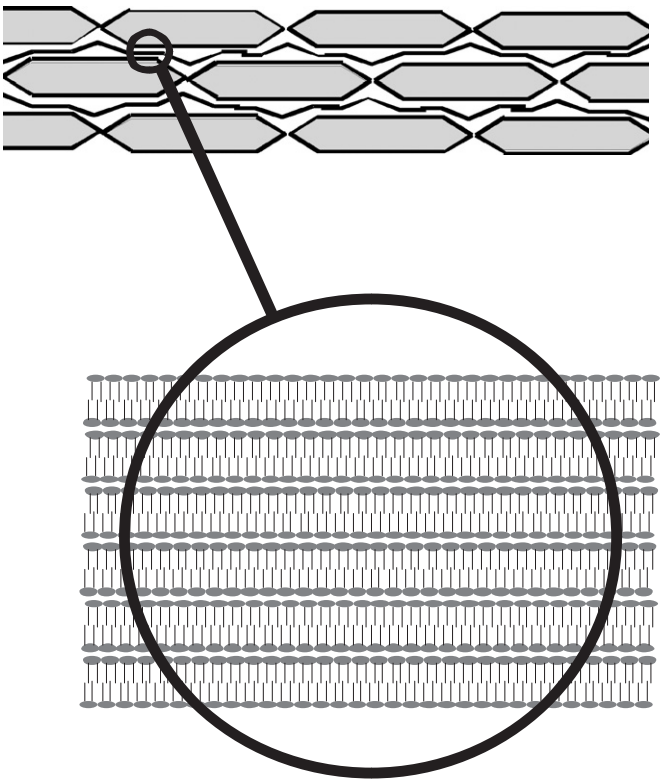

Fig. 1. Schematic of the stratum corneum. The flattened corneocytes have a thickness of 1 mm and a diameter of 10 mm. The multi-lamellar structure between adjacent corneocytes is magnified for better clearance. Each lipid layer has a thickness of proximately 4–7 nm depending on the hydration of the skin. The number of corneocyte layer and the lipid layers between them depends on the body location.

Since the heating within the very small electropores is not adiabatic, the temperature rise is limited by the pore size. Calculations taking heat transfer into account show a negligible temperature rise ($\Delta\vartheta < 1$ K) for pathways with a radius of 1 nm, which is the expected size of electropores in lipid bilayers (Martin et al., 2002). In order to account for the development of LTR just by heating, a small population of giant electropores ($r_{pore} > 10$ nm) is required.

If electroporation occurs stochastically within lipid layers of the SC an aqueous pathway will be formed, if all stacked layers are electroporated. The probability that this will occur increases with the field strength applied. However, this process provides no rationale to explain the experimental observation that an LTR increases in size for the duration of the pulse. The field strength in the immediate vicinity of an electropore is weakened, thereby reducing the probability of electroporation in this region. Only if the electroporated region is large, on the order of $r_{pore} = 50$ nm, would heat production be sufficient for lipid alterations. It seems possible that pre-existing defects of the SC such as the remnants of desmosomes are responsible for the creation of big pores. However, this requires additional assumptions which have yet to be verified, and which are beyond the scope of this paper. Our model requires no critical assumptions and is based exclusively on experimental results on whole SC.

The SC is a complex multi-layered structure (Elias, 1988). Since the density of LTR rises almost linearly with applied voltage difference between 60 and 120 V at room temperature, it was concluded that spots with a certain electroporation voltage (critical voltage for electroporation) show little variation across the skin surface (Pliquett et al., 1996). When the SC is charged up to a voltage between $60\,\text{V} < R_{skin} < 120\,\text{V}$, all regions with a lower electroporation threshold voltage will experience electroporation. The initial pores through the multi-lamellae are very small ($r_{pore} \approx 1$ nm) (Weaver et al., 1999). The critical pore radius at which the field reduction equals $1/e$ of the difference between the undisturbed field and the field within an electrically created pore is about 3 nm. With a corneocyte diameter of 10 μm, it is unlikely that the appearance of a single pore prevents further electroporation within the envelope of the same corneocyte.

Given a random distribution of defects or thinner regions of the lipids within the SC, it is plausible that electroporation sites will be clustered in some regions and would create a pathway much larger than a single pore. Independent simulations on the level of whole SC indicate that clusters form even if using random numbers but a Gaussian distribution is expected for the breakdown voltage of each skin patch. These clusters themselves differ in average breakdown voltage, which implies that with increasing applied voltage, the number of clusters forming permeable regions by electroporation will increase.

Joule heating takes place at electroporated sites. If a single pore is heated the heat transfer will prevent sufficient temperature rise for thermally forced field effects. However, rough approximation shows that if initial pores are clustered, forming a permeable region with a radius of more than 5 nm, a temperature increase of several Kelvin will occur. This will decrease the voltage necessary for electroporation within the immediate vicinity of the pore cluster and will create more electropores which results in an even greater heat production and thereby further appearance of electroporation at the edge of the permeable region. Because of this self-catalyzing process at the edge of permeable regions, a propagating heat front starts from the initial pore cluster. Since the heat transfer becomes small in the central region, the temperature at these sites increases further, exceeding even the phase transition temperature of the long-chain sphingolipids. During the dramatic decrease of the skin resistance, the transdermal voltage will decrease as well. However, this reduction in electric field is compensated by local heating, so that the development of the LTR will continue as long as the overall transdermal voltage is sufficiently high.

Once sphingolipids reach their phase transition temperature, they will break off the multi-lamellar structure and form aggregates (vesicles) with water-rich surfaces (Gallo et al., 2002). Along these surfaces aqueous pathways large enough to accommodate molecules as large as DNA will be formed. When the pulse ceases, the SC cools down within milliseconds, which is detected electrically as an increase of the skin resistance by more than one order of magnitude. As evident from experiments, two distinct regions appear: (1) the region where phase transition occurred and the multi-lamellar system is compromised and (2) the region where electroporation and heating just decreased the skin resistance without destruction of the lipid conformation. The recovery of the electric resistance within the first region is negligible, while the rest recovers to almost 100% of the pre-pulse value.

3. Simulation

The pore radius calculated from experimental data cannot account for a pore spanning the whole SC. This means that the critical part of our hypothesis is that the field acts on the level of the multi-lammelar lipid sheets between adjacent corneocytes, which we were unable to resolve experimentally.

The electroporation of skin is a complex phenomenon and our mathematical description takes into account the electrical changes within the SC. These include the interaction between heating and probability of electroporation and the changes in the electric field distribution within the bathing saline. The simulation focuses on the interaction between electric field and heating on the level of the multi-lamellar lipid sheets (Fig. 1) with a thickness of 30 nm. The simulation itself is carried out by numerically solving differential equations (heat transport equation and the electric field distribution) using finite elements.

3.1. Model

Electroporation takes place within the multi-lamellar system of sphingolipids. As typical for the human SC, the model contains six lipid bilayers, surrounded by water. Given the thickness of one layer of 5 nm, the lipid structure has a thickness of 30 nm. The voltage across the skin drops mostly across the lipid layers. Since about 6–10 corneocytes are in series with 6–10 lipid bilayers in between, the final number of lipid layers varies between 40 and 100, depending on body location. Thus, the voltage across the lipid system between adjacent corneocytes is 6–20 times less than the voltage applied across the SC.

The model contains volume elements with fixed dimensions. The dimensions within the multi-lamellae are $1 \times 1 \times 30\,\mathrm{nm}^3$, which allows the simulation of pores as small as 1 nm in diameter. The lipid phase is modeled as a continuum instead of a multi-lamellar system. In order to minimize calculation time, we only modeled single pores with square cross section which yields cuboid-like pores. Clusters of electropores are modeled as permeable regions with homogeneous conductivity. A volume element within the bathing saline has the same lateral dimensions as the lipid elements but a vertical length of 1 nm. The time grid of the simulation is 1 ps. The simulation uses cyclic calculation of the field distribution, the Joule heating, the electric conductivity change of electrolytes as well as the heat redistribution due to heat flow. The program allows changing the parameter for each volume element during simulation. The simulation uses ideal heat sink condition at the edges of the simulation space, justified by the size of corneocytes which is at least two orders of magnitude larger than the influence radius of a heated pore.

The simulation package is written in MATLAB 5 (The MathWorks Inc., Natik, MA). Since MATLAB is optimized for handling matrixes, all calculations use matrix operations. The initial parameters are set as listed in Table 1.

3.2. Initial step: the creation of permeable regions

Each volume element of the lipid matrix has its unique breakdown voltage between 6 and 10 V with a Gaussian distribution. The simulation takes into account the charging of the skin at various current densities. Once the electroporation condition of one element is reached, the volume element turns into an aqueous pathway and gives rise to the distortion of the electric field within the bathing saline. If enough pores are created the voltage cannot increase further. This simulation should be understood as a rough estimation and does not take the energy for pore formation into account. The result is a pattern of aqueous pathways in which most are single pores but others show clusters, where the density of these clusters is a function of current density as it was found experimentally and by simulation for the whole SC. This part of the simulation is separated from the rest and is used to demonstrate the probability of appearance of large permeable regions, even if the critical parameters for electroporation have a Gaussian distribution over the surface. Unfortunately, for this step clear experimental results on the membrane level are still lacking. In order to ensure comparable results for subsequent steps, a pore with defined dimension was created in the middle of the simulation space.

Table 1
Parameters used for simulation

Initial temperature (°C)	25
Initial conductivity within a single pore (S/m)	0.7
Initial conductivity of the saline (S/m)	1.4
Density of saline (kg/m^3)	1000
Density of lipids (kg/m^3)	900
Heat capacity of saline (J/(kg K))	4170
Heat capacity of lipids (J/(kg K))	1800
Heat conductivity of water (W/(m K))	0.58
Heat conductivity of lipids (W/(m K))	0.2

3.3. Electric field

The electric field is calculated for each volume element within the lipid layer and the bathing electrolytes by taking the spreading resistance and the conductivity of the specific volume element into account.

3.4. Heat production

The temperature increase within the time raster for each element was calculated by $\Delta\vartheta = (E^2\kappa\Delta t/\rho c)$, where $\Delta t = 1$ ps is the spacing of the time vector. E is the electric field strength, κ the conductivity, ρ the mass density and c is the specific heat capacity of the individual volume element.

3.5. Heat transfer

The heat transport equation is solved in one dimension and applied in six directions (three coordinates both backward and forward). The influence of convection was neglected because experiments using tritiated water indicate that the rate of water exchange, i.e. the convection has a very small influence on the temperature change of less than 10% (Pliquett et al., 2002).

3.6. Conductivity

Because of large temperature variations inside the pores (25–100 °C), the temperature dependence of conductivity needs to be taken into account. Here, a temperature coefficient of 2.7%/K with respect to 25 °C was used (experimental data). The conductivity of the lipids was always set to zero.

3.7. Probability of electroporation

A matrix was created with Gaussian distributed voltages necessary for electroporation at 25 °C. This initial matrix was updated due to the heating of each volume element within the lipid environment using experimental data for the critical electroporation voltage of the entire SC. Once the conditions for electroporation for one element were reached, the element's conductivity was switched to the conductivity of saline at the specified temperature for further steps in the simulation.

3.8. Simulation results

The temperature rise within a permeable region is a function of its dimensions, the voltage drop across it, the duration of the applied voltage and the heat transfer. Fig. 2 illustrates the lateral temperature distribution for $100 \times 100\,\mathrm{nm}^2$ region of the multi-lamellar system between adjacent corneocytes. The boundaries of this region are modeled as perfect heat sinks with zero conductivity (lipids).

The temperature increases until a steady state between heat production and heat transfer across the boundaries of the permeable region is reached. Fig. 3 shows how this final temperature depends on the pore radius. It should be noted that this is only approximately the radius because of the square cross section of the initial pore.

The temperature gradient at the edge of the permeable region ranges between 10^6 and $10^9\,\mathrm{K/m}$ (Fig. 4), which limits the influence of elevated temperature to the immediate vicinity. Very similar results were found experimentally on the scale of the whole SC (Pliquett and Gusbeth, 2000). Based on this result, it is clear that heating alone cannot be responsible for the propagating heat front observed in experiments.

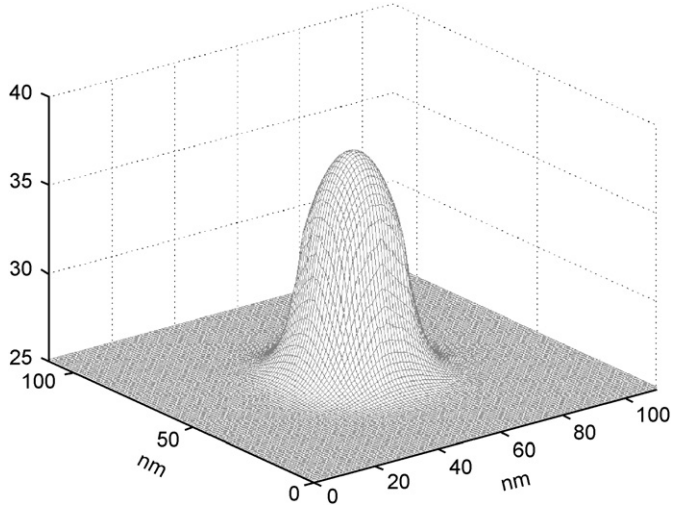

Fig. 2. Temperature distribution in the vicinity of a permeable region ($r = 10\,\mathrm{nm}$) within the multi-lamellar system between adjacent corneocytes after 1 ns. The voltage across the lipid layer is 10 V and the initial temperature is 25 °C. The field digression due to the lowering of the membrane resistance is taken into account; however, the probability of further electroporation is set to zero.

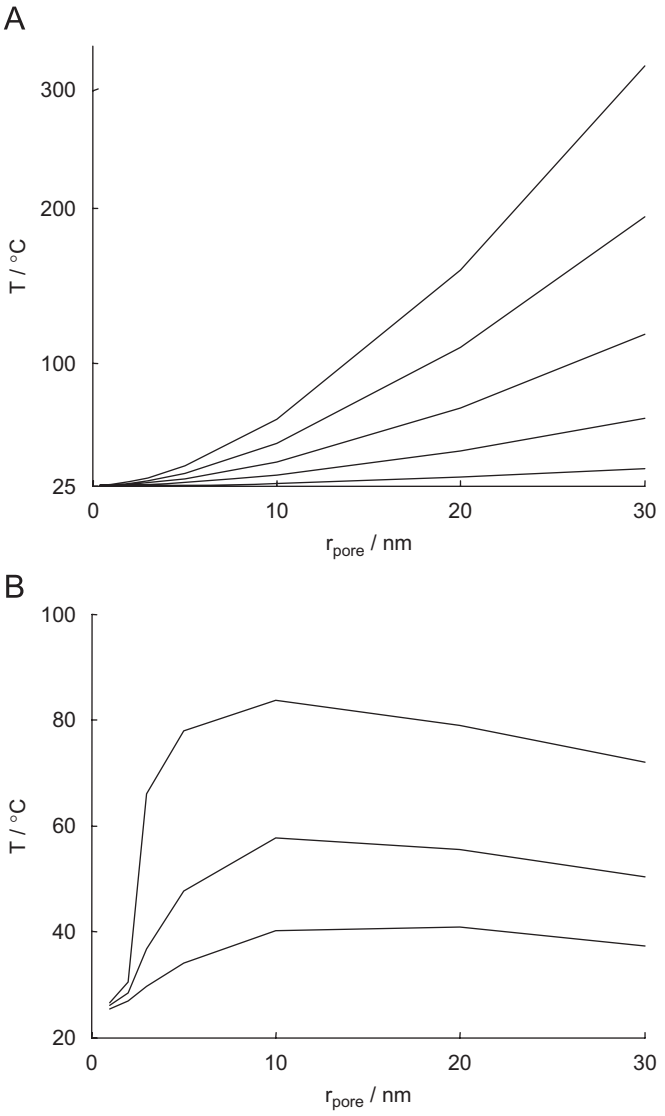

Fig. 3. Equilibrium temperature rise within a permeable region depending on its radius assuming a constant field strength. (A) Analytical calculation without heat sink at the boundaries and with constant voltage (6, 8, 10, 15, 20 V, from bottom to top). (B) More realistic numerical simulation by modeling an infinite heat sink in a distance of five times the pore radius r_{pore} at 25 °C. Moreover, a more realistic electric field distribution based on the voltage divider between the lipid structure and the saline is taken into account (6, 8, 10 V, from bottom to top).

The temperature rise occurs very rapidly but levels off rapidly as well (Fig. 5). If the dimension of the permeable region is held constant (no further electroporation allowed), the achievement of the steady state condition takes only nanoseconds for reasonable initial conditions.

The high conductivity of a permeable region distorts the electric field pattern in that region. The radius of influence of this disturbance is determined by the spreading resistance. It becomes increasingly important with increasing pore radius. The influence radius for the small initial pores ranges between 3 and 10 nm (Fig. 6), enough to

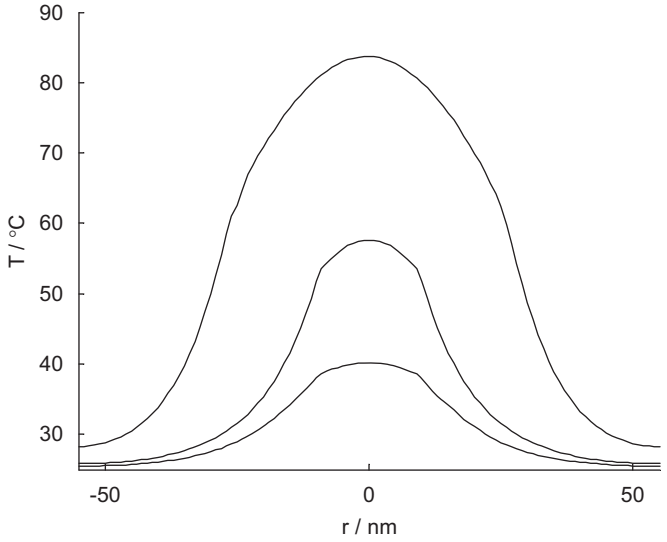

Fig. 4. Temperature profile in the immediate vicinity of a permeable region ($r_{pore} = 10$ nm) 10 ns after pulse trigger. The probability of electroporation was set to 0, so that only heating from initial pathways occurs. The voltage applied was 6, 8 and 10 V, from bottom to top.

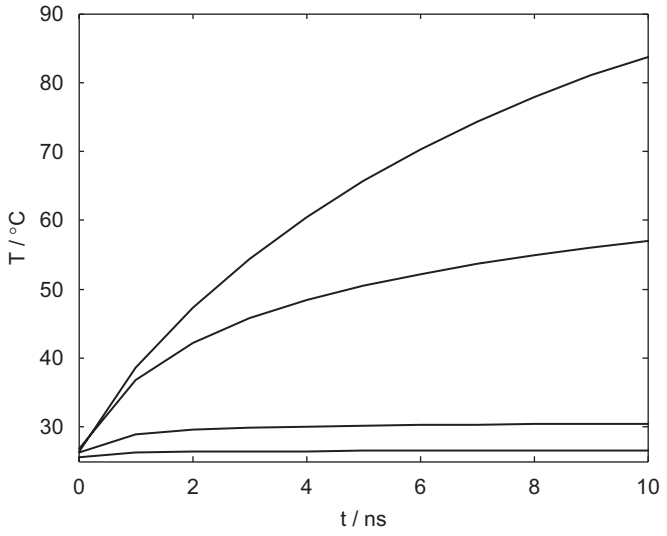

Fig. 5. Temperature within a permeable region within 10 ns after voltage is applied. The pore radius is from bottom to top: 1, 2, 5 and 10 nm. No charging time is considered and the geometry of the pore remains unchanged. The voltage across the lipid structure between adjacent corneocytes with 5 nm saline above and below is 10 V.

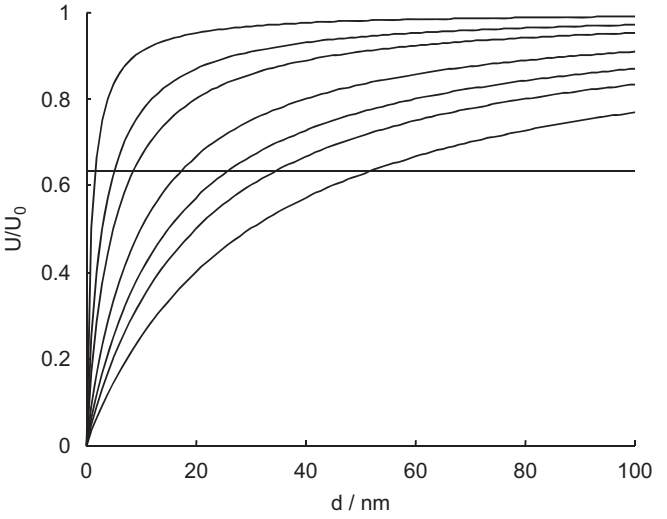

Fig. 6. Transmembrane voltage distortion as a function of distance d from the edge of a permeable region for different pore radii (beginning on the left: 1, 2, 5, 10, 15, 20, 30 nm). The actual potential is normalized to the potential of the far electrode and the surface of the permeable region ($\varphi = 0$). The line at $\varphi_{rel} = 0.63$ indicates the criteria for the influence radius.

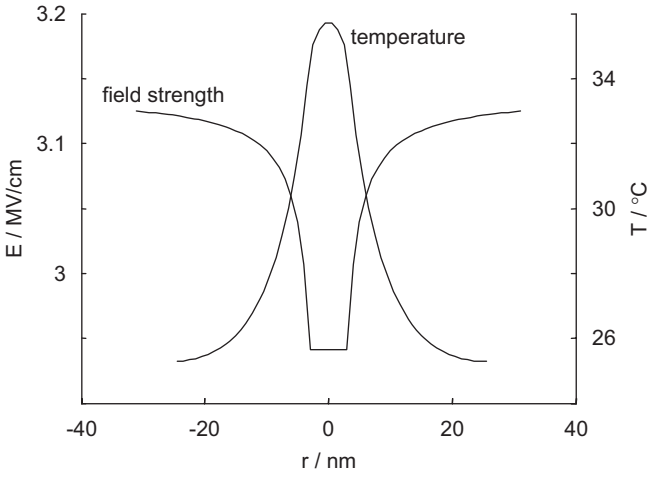

Fig. 7. Local distribution of elevated temperature and distortion of the electric field by the spreading resistance after 10 ns. The radius of the permeable region was 2.5 nm.

disturb the field around the pore but not enough to prevent multiple electroporation sites within the same corneocytes within a diameter of about 15 μm. However, the decreased field around a permeable region prevents electroporation at the edges, which would also prevent the growth of the electroporated region as is experimentally observed. Our simulation results show that neither the heating nor field effect alone is able to form LTRs. Only with additional conditions, like pre-existing defects within the SC or a very large applied voltage can LTRs possibly develop.

If the decrease in critical transdermal voltage at elevated temperature is taken into account, some spots around the edges of permeable regions will experience electroporation. As shown in Fig. 7, there is a small region at the periphery of the permeable region experiencing the elevated temperature but at a distance from the existing permeable region so that the electroporation condition is achieved.

This increases the heat production in this region and results in a propagating heat front. Fig. 8 shows the emerged initial region 200 ns after voltage application.

The influence of energies like pore energy, energy stored in the charged membrane or curvature energy by introduction of water into the membrane structure, are not taken

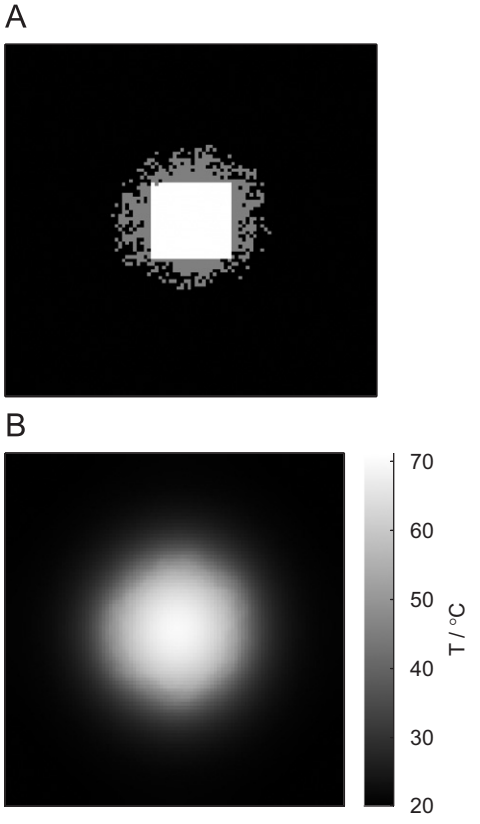

Fig. 8. Permeable region 5 ns after the application of 10 V. (A) The initial area was $30 \times 30\,nm^2$ (white square) approximating a radius of 15 nm. Electroporation was allowed, i.e. when the electroporation conditions for a volume element were achieved. The conductivity of this element was set to the pore conductivity (gray). (B) The interior of the permeable region experiences temperatures well above the phase transition temperature of the lipids (70 °C).

into account, making this simulation a rough estimation, but showing the basic features of skin electroporation.

4. Summary

High voltage application at lipid multi-layers yields highly localized electroporation. This localization can be observed stochastically and does not need pre-existing defects. The development of large permeable regions is the result of synergistic interactions between electric field effects and heating. It is assumed that after initial pore creation further electroporation takes place at the heated edges of initial pore clusters. The energy dissipation inside the propagating heat front yields temperatures above the phase transition of the skin lipids. This yields an LTR, a region with an extremely high permeability for water-soluble compounds. The electric resistance of these regions does not recover, as is characteristic for multi-lamellar sheets exceeding the phase transition temperature.

Acknowledgments

This work was supported by the Deutsche Forschungsgemeinschaft, Pl-185/2,3 to U.P. We thank T. Vaughan, G. Martin, J. Weaver, Y. Chizmadshev and F. Pliquett for helpful discussions.

References

Chizmadzhev, Y.A., Zarnitsin, V.G., Weaver, J.C., Potts, R.O., 1995. Mechanism of electroinduced ionic species transport through a multilamellar lipid system. Biophys. J. 68, 749–765.

Elias, P.M., 1988. Structure and function of the stratum corneum permeability barrier. Drug Dev. Res, 97–105.

Gallo, S.A., Sen, A., Hensen, M.L., Hui, S.W., 2002. Temperature-dependent electrical and ultrastructural characterization of porcine skin upon electroporation. Biophys. J. 82, 109–119.

Glaser, R.W., Leikin, S.L., Chernomordik, L.V., Pastuchenko, V.F., Sokirko, A.I., 1988. Reversible electrical breakdown of lipid layers: formation and evolution of pores. Biochim. Biophys. Acta 940, 275–287.

Martin, G.T., Pliquett, U., Weaver, J.C., 2002. Theoretical analysis of localized heating in human skin subjected to high voltage pulses. Bioelectrochemistry 57, 55–64.

Neumann, E., Sowers, A., Jordan, C., 1989. Electroporation and Electrofusion in Cell Biology. Plenum Press, New York.

Pliquett, U., Gusbeth, C., 2000. Perturbation of human skin due to application of high voltage. Bioelectrochem. Bioenerg. 51, 41–51.

Pliquett, U., Langer, R., Weaver, J.C., 1995. Changes in the passive electrical properties of human stratum corneum due to electroporation. Biochim. Biophys. Acta 1239, 111–121.

Pliquett, U., Zewert, T.E., Chen, T., Langer, R., Weaver, J.C., 1996. Imaging of fluorescent molecule and small ion transport through human stratum corneum during high-voltage pulsing: localized transport regions are involved. Biophys. Chem. 58, 185–204.

Pliquett, U., Vanbever, R., Weaver, J.C., 1998. Local transport regions (LTRs) in human stratum corneum due to long and short high voltage pulses. Bioelectrochem. Bioenerg. 47, 151–161.

Pliquett, U., Martin, G.T., Weaver, J.C., 2002. Kinetics of temperature rise within the stratum corneum during electroporation and pulsed high voltage electrophoresis. Bioelectrochemistry 57, 65–72.

Prausnitz, M.R., Bose, V.G., Langer, R., Weaver, J.C., 1993. Electroporation of mammalian skin: a mechanism to enhance transdermal drug delivery. Proc. Natl Acad. Sci. (USA) 90, 10504–10508.

Prausnitz, M.R., Gimm, J.A., Guy, R.H., Langer, R., Weaver, J.C., Cullander, C., 1996. Imaging regions of transport across human stratum corneum during high voltage and low voltage exposures. J. Pharm. Sci. 85, 1363–1370.

Vanbever, R., Pliquett, U., Weaver, J.C., 1999. Transdermal transport and changes in skin electrical properties due to short and long high voltage pulses. J. Control Release 60, 35–47.

Weaver, J.C., Chizmadzhev, Y.A., 1996. Electroporation. In: Polk, C., Postow, E. (Eds.), CRC Handbook of Biological Effects of Electromagnetic Fields. CRC Press, Boca Raton, pp. 247–274.

Weaver, J.C., Vaughan, T.E., Chizmadzhev, Y.A., 1999. Theory of electrical creation of aqueous pathways across skin transport barriers. Adv. Drug Deliv. Rev. 35, 21–39.